JOURNAL OF THERMOPHYSICS AND HEAT TRANSFER
Vol. 24, No. 2, April–June 2010

Statistical Model for Pressure Distribution of Bolted Joints

Marcia B. H. Mantelli,* Fernando H. Milanez,† and Eliete N. Pereira‡
Federal University of Santa Catarina, Florianopolis, 88040-900 Santa Catarina, Brazil
and
Leroy S. Fletcher§
Texas A&M University, College Station, Texas 77843-1265

DOI: 10.2514/1.42198

This paper proposes the use of the Weibull probability density distribution to predict the shape of the contact pressure distribution in bolted metal joints. Contact pressure distributions in bolted joints were measured using a commercially available pressure-sensitive film. Three different joint materials were analyzed: aluminum–aluminum, stainless steel–stainless steel, and aluminum–stainless steel. The metal plates were circular and bolted together through a hole at their center. Two bolt head radii were employed. Five different axial loads were applied for each bolted joint configuration. The agreement was very good between the correlations, based on the Weibull distribution and the data. The results indicate that the Weibull function is an adequate model for the shape of the contact pressure distribution of bolted joints.

Nomenclature

a	=	bolt hole radius, m
b	=	bolt head radius, m
$b1$	=	5 mm bolt heat radius
$b2$	=	9 mm bolt head radius
c	=	contact radius, m
F_a	=	axial force, N
J_{lmn}	=	joint configuration for which l is the applied load, m is the joint material, and n is the bolt size
P_a	=	average axial pressure, Pa
r	=	coordinate axis from the bolt centerline, m
t	=	plate thickness, m
α	=	contact cone angle, deg
β, η, ρ	=	Weibull parameters

Introduction

THIS work deals with the contact pressure distribution in bolted joints. One of the several applications of bolted joints is the thermal control system of microelectronic devices aboard spacecraft and satellites. The pressure distribution between the contacting surfaces in bolted joints plays a very important role in modeling the thermal contact conductance. If the contact pressure distribution between the surfaces is uniform along the interface of the bolted joint, the contact conductance could be calculated using theoretical results or correlations actually available in the literature. Many authors, such as Fernlund [1], Motosh [2,3], Chandrashekhara and Muthanna [4–6], and Marshall et al. [7] show that the pressure reaches a peak near the bolt and drops to zero in a distance of a few radii away from the bolt centerline. Depending on the applied load, the contact may even be lost in regions away from the bolt, as illustrated in Fig. 1.

Received 14 November 2008; revision received 3 December 2009; accepted for publication 11 January 2010.

*Professor, Department of Mechanical Engineering, Heat Pipe Laboratory; marcia@emc.ufsc.br. Associate Fellow AIAA.
†Research Engineer, Department of Mechanical Engineering, Heat Pipe Laboratory; milanez@labtucal.ufsc.br.
‡Research Assistant, Department of Mechanical Engineering, Heat Pipe Laboratory.
§Professor, Department of Mechanical Engineering, 314 Engineering/Physics Building Office Wing.

The main objective of this study is to show that the contact pressure distribution of bolted joints is well described by the Weibull probability density function. Pressure distribution data, collected using pressure sensitive films, are employed. Six different bolted joint configurations subjected to five different axial loads are studied.

Literature Review

The open literature presents several numerical and analytical models to predict pressure distribution of bolted joints. Experimental studies can be found as well. The analytical models calculate the pressure distribution as a function of the contact radius c (see Fig. 2) (i.e., the distance from the bolt centerline at which the contact pressure distribution drops to zero). The contact radius is, in turn, a function of the contacting plate thicknesses t_1 and t_2, the contact cone angle α, and the bolt head radius b.

According to Fernlund [1], Rötsher was one of the first researchers to calculate the contact radius of two plates in a bolted joint. He considered that the joint stress disperses within a frustum of a 45 deg semiangle (see α in Fig. 2). He also considered that the interfacial pressure is constant within the contact radius c. This hypothesis was the first approximation for the contact radius, but the pressure distribution was not described satisfactorily.

Fernlund [1] developed an analytical method based on the elasticity theory to obtain the pressure distribution on the interface of two bolted plates as a function of the radius. He used a Hankel transform method and modeled two plates with the same thicknesses and the same materials as a single plate with double thickness. The contact pressure between the two plates was assumed to be equal to the normal stress at the mean plane of the single plate. As the result was difficult to apply, an approximate method was proposed, for which the contact pressure was represented by a fourth-order polynomial, which is a function of the dimensionless radius r/a.

Gould and Mikic [8] investigated the pressure distribution and the contact radius using the finite-element method. They analyzed single- and double-plate models in several different geometric configurations. The comparison between their results shows that the contact radius calculated applying the double-plate model is significantly lower than that of the single-plate model. They also studied joints with plates of equal and of different thicknesses and concluded that the contact radius between the plates with different thicknesses is lower than that of plates of the same thicknesses.

Chandrashekhara and Muthanna [4–6] developed an analytical solution in terms of the Fourier–Bessel series for a thick plate with a circular hole in its center and submitted to an axisymmetric compression load. Various t/a and b/a ratios were considered for material with different values of the Poisson coefficient. The results

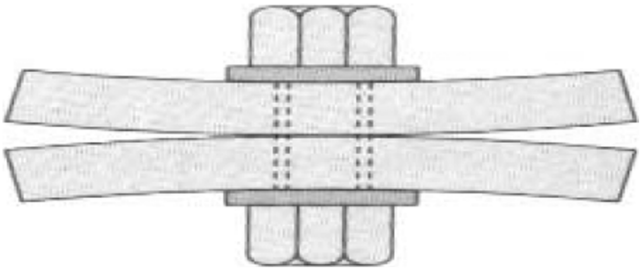

Fig. 1 Illustration of plate separation in a bolted joint (exaggerated).

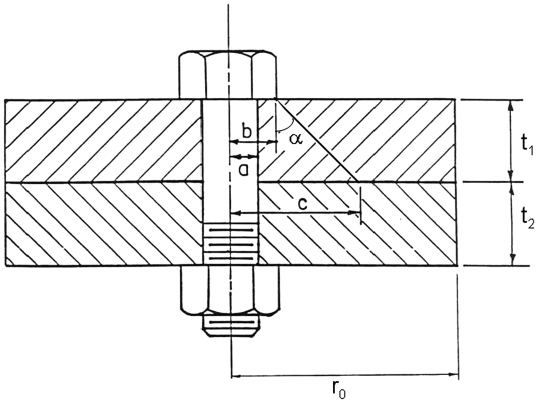

Fig. 2 Bolted joint geometry.

showed that the pressure in the interface tends to zero for $r/a > 5$. They also observed that, for elastic deformation, the only material property that can affect the pressure distribution was the Poisson coefficient.

Madhusudana et al. [9] proposed three different pressure distributions for bolted plate joints: linear, parabolic, and polynomial (depending on the plate thicknesses, the bolt hole radius, and the bolt head).

Regarding the contact pressure measurements in bolted joints, two main techniques have been employed in past works: interface ultrasonic waves reflection and pressure-sensitive films. The first is more accurate, whereas the second is much easier to perform. Ito et al. [10] measured the interfacial pressure distribution on bolted flanges by means of ultrasonic waves. The authors showed that the surface roughness, the material, and the thickness of the plates influence the pressure distribution and the contact radius. Semihard stainless steel (S45C), brass (BsBM1), and aluminum (AlB1) plates were investigated with applied axial forces varying from 9.8 to 19.6 kN. The authors concluded that the smaller the plate thickness, the higher the pressure levels. Marshall et al. [7] also employed an ultrasonic waves reflection technique to measure the interface pressure in bolted joints. They tested the ground and the turned surfaces and found that the surface roughness significantly affects the pressure distribution.

Mittlebach et al. [11] measured the pressure distribution using a commercially available pressure-sensitive film to study both the interfacial pressure distribution and the thermal conductance of bolted joints. The film was the same as the one used to obtain the data presented here. The variables considered by those researchers were bolt torque (axial force), plate thickness, and interface average temperature. They studied the joints composed by plates of aluminum (6061-T6) with an outer radius of 45.7 mm, $b/a = 1.6$, and with a ratio thickness t_2/t_1 of 19.1/19.1, 12.7/19.1, and 25.4/19.1 mm. The axial load varied from 6.69 to 13.425 kN. They compared various pressure distribution models from the literature against their experimental data and concluded that the models of Chandrashekhara and Muthanna [5] and of Fernlund [1] agreed best with the data. Also, they verified that the peak pressure value of Chandrashekhara and Muthanna's [5] model was higher than that of Fernlund's [1] model.

The pressure-sensitive film was also used by Pau et al. [12], who also employed the ultrasonic waves technique and concluded that there is substantial agreement in terms of the sizes and shapes of the contact areas between the two methods. Sawa et al. [13] measured the contact pressure distribution of a bolted joint with a different geometry from the one shown in Fig. 2. Instead of two plates, they used a bolt inserted into a threaded hole body of a larger body. The bolt was used to fasten a clamped part, which was basically a hollow cylinder, to the body. Metal gaskets were inserted between the clamped part and the body. The measurements were made using three different techniques: pressure-sensitive films, ultrasonic waves, and pressure-sensitive pins. They also developed a numerical model to predict the contact pressure distribution. They found a fairly good agreement between the measurements and the analytical results. They concluded that the method with the pressure-sensitive films was the simplest. However, it did not work well when the stiffness of the clamped part and the body were large. But, when an aluminum gasket was employed, the measurement was consistent with the numerical results. The authors also concluded that the sensitive pins and the ultrasonic waves were very complicated, because smooth contact surfaces had to be obtained.

Bolted Joint Pressure Distribution Data

An experimental study on the pressure distribution of contacting surfaces of two plates fastened by a bolt was conducted at the Conduction Heat Transfer Laboratory of Texas A&M University. A pressure-sensitive film, manufactured by the Fuji Corporation, was used that consisted of two contacting sheets: one containing a thin layer of microcapsulated ink bubbles and the other containing a layer of color-developing material. When the films are forced against each other, some of the microcapsules are broken up, dying the other sheet. The color density on the developing sheet then reveals the pressure distribution. The color density is scanned by a densitometer, which is manufactured by the same company as the sensitive films. The color density is then converted into pressure distribution values.

According to the manufacturer, the precision of pressure measurements with this method is $\pm 10\%$. However, to verify the accuracy of the pressure-sensitive films, the pressure distribution data were also compared against the total load applied by the bolt, which was measured by means of a load cell located between the lower plate and the bolt head. Figure 3 shows a schematic of the experimental setup. Apart from the pressure distribution measurements, the experimental setup was also used for thermal contact resistance measurements. The electric heater and the cold-plate heat sink used in the thermal measurements are also depicted in Fig. 2. However, the thermal contact conductance study is not included in the present work.

The measurements were made on bolted joints made of three different combinations of materials: aluminum 6061/aluminum 6061, stainless steel 304/stainless steel 304 and aluminum 6061/stainless steel 304. The bolted joints were made of nominally flat and smooth

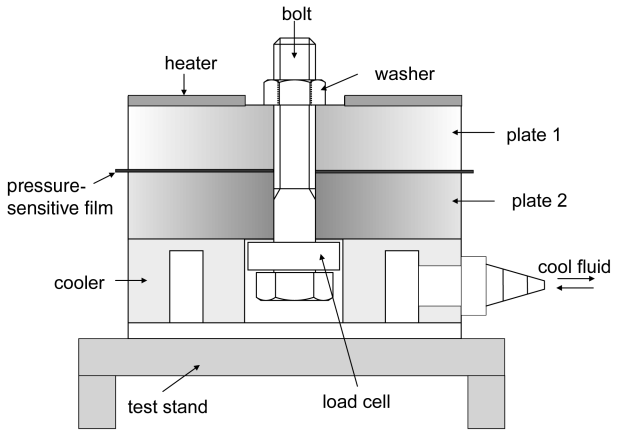

Fig. 3 Schematic of test setup.

Table 1 Test summary

	5 mm bolt head radius			9 mm bolt head radius		
Axial force, N	Al–Al	SS–SS	Al–SS	Al–Al	SS–SS	Al–SS
1624	J111	J121	J131	J112	J122	J132
3247	J211	J221	J231	J212	J222	J232
6672	J311	J321	J331	J132	J322	J332
12,233	J411	J421	J431	J412	J422	J432
18,371	J511	J521	J531	J512	J522	J532

circular plates with a 46 mm outer radius. The thicknesses were 19 and 13 mm for the aluminum and the stainless steel plates, respectively. The plates were lapped, and the RMS surface roughness was found to be less than 3.7 μm. The screw-hole radius was 3 mm. Two different bolt head sizes were tested: 5 and 9 mm radii. The axial forces of 1624, 3247, 6672, 12,233, and 18,371 N were tested for each joint configuration. Table 1 shows a list of all the tests performed. The tests are labeled as J_{lmn}, where l is the axial force applied, m is the joint material combination [(aluminum–aluminum (Al–Al), stainless steel–stainless steel (SS–SS), or aluminum–stainless steel (Al–SS)], and n is the bolt head radius (1 for 5 mm and 2 for 9 mm).

Before using the pressure distribution data to develop correlations, the accuracy of the pressure-sensitive film was checked by numerically integrating the measured pressure distributions over the contact area. The results were then compared with the respective measured load cell readings. The integration of the pressure distribution yielded values up to 70% larger than the load cell measurements. As the load cell was previously calibrated, the authors concluded that pressure-sensitive films do not give accurate values of pressure levels. Also, the pressure measurements did not vanish far from the bolt as expected, which indicates a bias error. However, the overall shape of the pressure distribution curve seemed to be right. The authors then decided to introduce corrections to the measured pressure distributions, so that they vanished far from the bolt, and their integration over the contact area yielded the total axial force read by the load cell. The corrections were introduced in two steps: 1) subtract a constant value from the pressure distribution, so that the pressure vanishes far from the bolt and 2) multiply the curve by a constant factor, so that the integration of the final distribution yields the measured applied load. In other words, we keep the shape of the pressure distribution curve captured by the pressure-sensitive films and adjust the amplitude of the distribution, so that the total force matches the load cell reading. Despite the pressure measurements showing that the sensitive film did not give accurate values of the absolute pressure levels, it is appropriate for the objective of this work, which is to study the shape of the pressure distribution.

Comparison Between Experimental Data and Literature Models

In this section, the pressure distributions obtained using the models of Fernlund [1] and of Madhusudana et al. [9] are compared against the Al–Al and SS–SS collected data. The models are not compared with the Al–SS data, because the models are only valid for joints of the same material. All the data points and the literature models were made dimensionless by dividing them by the average axial pressure. The average axial pressure is obtained by dividing the axial force (load cell) by the bolt head area in contact with the upper plate, which is an annulus of the outer radius b and the inner radius a; that is,

$$P_a = \frac{F_a}{(b^2 - a^2)\pi} \tag{1}$$

The literature models are based on the knowledge of the contact radius, which is calculated here using Rötscher's model:

$$c = b + t(\tan\alpha) \tag{2}$$

This result can be easily derived from Fig. 2. Chandrashekhara and Muthanna [5] proposed a model for the semiangle α as a function of the ratio d/a. For the type of joints analyzed in this work, the value is larger than 50 deg. Figures 4–6 show the comparison between the data and the model that presented the best agreement. In these figures, the following nomenclature is adopted: Fe denotes Ferlund's [1] model followed by the value of α.

Figure 4 shows the dimensionless pressure data obtained for the Al–Al joints, submitted to five different levels of axial load. This figure also shows the pressure distribution obtained by Fernlund's [1] model, using an angle of $\alpha = 60$ deg and a 5 mm bolt head radius. The data of the Al–Al joint with the 9 mm bolt head radius and Fernlund's [1] model with an angle of 55 deg are presented in Fig. 5. The agreement is reasonable, although Fernlund's [1] model suggests that all the dimensionless data should collapse on the same curve, regardless of the absolute value of the axial load. However, this was not observed from the experimental data, especially near the bolt region.

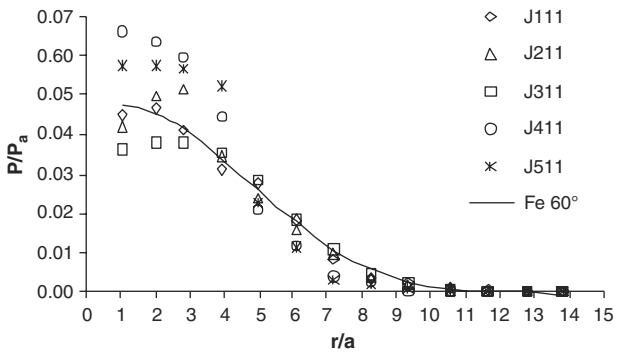

Fig. 4 Fernlund [1] model with $\alpha = 60$ deg and data from Al–Al with a 5 mm bolt head radius.

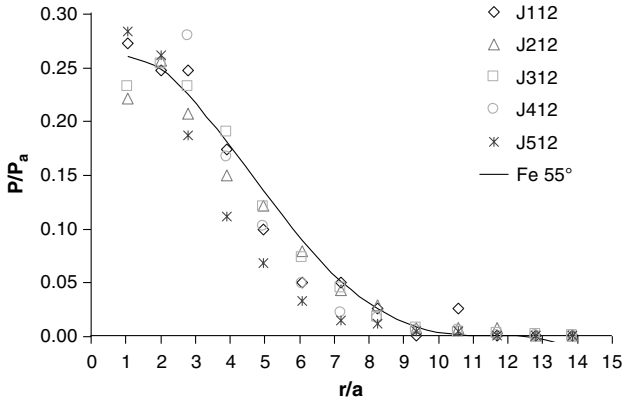

Fig. 5 Fernlund [1] model with $\alpha = 55$ deg and data from Al–Al with a 9 mm bolt head radius.

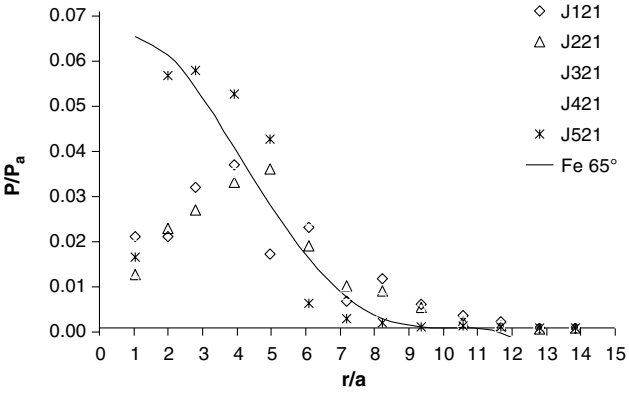

Fig. 6 Fernlund [1] model with $\alpha = 65$ deg and data from SS–SS with a 5 mm bolt head radius.

The joint between the two stainless steel plates with the 5 mm bolt head radius best compares with Fernlund's [1] model with $\alpha = 60$ deg and is shown in Fig. 6. The model does not capture the measured pressure gradient near the bolt well. The same comments made previously to the Al–Al joints regarding the collapsing of the data are valid for the SS–SS joints, but the agreement is not as good now.

Statistical Model

A new correlation is proposed here for the interfacial pressure distribution between two plates on a bolted joint. This correlation is based on the Weibull density probability function. The Weibull distribution is used in many fields, such as life data analysis, life tests engineering (Meyer [14]), and survival analysis, among other areas. It is related to the probability of failure of the parameter under observation, such as human life (death), breakdown of a mechanical structure, etc.

The general expression of the Weibull function is mathematically defined as

$$f(T) = \frac{\beta}{\eta}\left(\frac{T-\gamma}{\eta}\right)^{\beta-1} e^{-[(T-\gamma)/\eta]^{\beta}} \tag{3}$$

In this function, T is the independent variable (for example, life time or, as in this work, distance from the bolt centerline). The parameter that defines the curve shape is β: for $\beta \leq 1$, the curve has a negative slope, and for $\beta > 1$, the curve has both positive and negative slopes (i.e., presents a maximum value). The scale parameter is η, which gives the amplitude of the curve, and γ is the displacement parameter (i.e., the curve position relative to the vertical axis). These parameters are defined within the following ranges: $f(T) \geq 0$, $T \geq \gamma$, $\beta > 0$, $\eta > 0$, and $-\infty < \gamma < \infty$. When the displacement parameter is equal to zero, as in the present study, the resulting function is the Weibull distribution of two parameters. This distribution could be further reduced to just one parameter when either the shape parameter β or the scale parameter η are fixed.

The Weibull distribution is employed here to describe the contact pressure distribution measured with the pressure-sensitive films at the interface between the bolted plates. As the ink bubbles are adjusted to explode at different pressure levels, the color intensity could be seen as the probability of an amount of microcapsulated ink bubbles to explode (end of life), dyeing the color-developing sheet.

The Weibull distribution function employed here is multiplied by another parameter (ρ), so that the curve integration over the contact area yields the total force measured by the load cell readings. As already mentioned, the displacement parameter is zero, and the resulting equation used in this work (based on the Weibull distribution of two parameters) as a function of r is given by

$$f(r) = \rho\frac{\beta}{\eta}\left(\frac{r}{n}\right)^{\beta-1} e^{-(r/n)^{\beta}} \tag{4}$$

The pressure distribution data were correlated according to this function. In essence, a computer routine looked for the best values of β, η, e, and ρ (i.e., values that lead to the best possible agreement between the data and correlation).

Figures 7–12 show the Weibull distribution curves (lines) fitted to experimental data (symbols) for all the bolted joint configurations studied. Figures 7 and 8 show the comparison between the Weibull curves and the experimental data of the Al–Al joints for the 5 and 9 mm bolt head radii, respectively. In general, one can observe a very good agreement, indicating that the Weibull distribution is appropriate to the shape of the pressure distribution curve. For light load levels, the comparison between the data and the model is excellent. As the bolt axial load increases, the agreement gets a bit worse near the bolt: the model predicts a rapid slope change, whereas the data points suggest a smoother slope variation.

The comparison between the correlations and the experimental data for the SS–SS bolted joints are shown in Figs. 9 and 10, for bolt head radii of 5 and 9 mm, respectively. As also observed in the previous data sets, the models and the experimental data present an

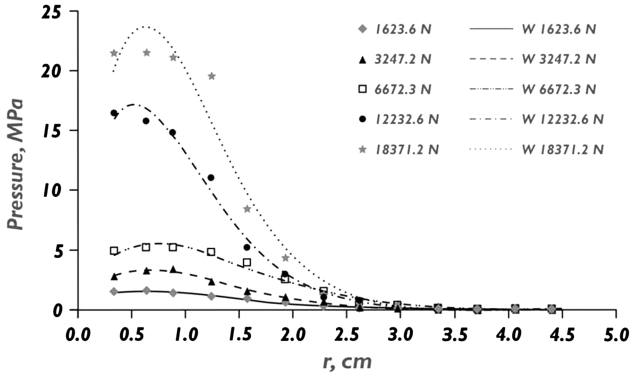

Fig. 7 Adjustment of Weibull curves for Al–Al with a 5 mm bolt head radius.

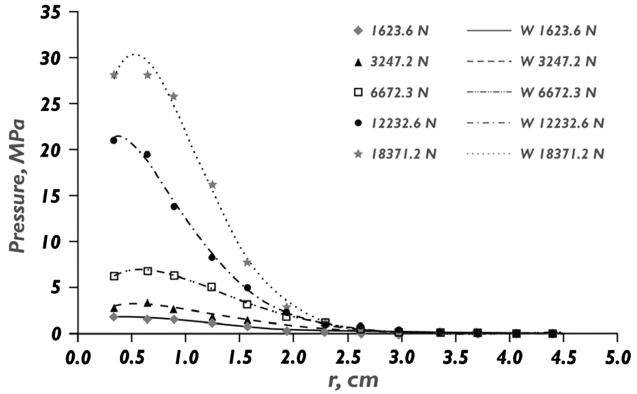

Fig. 8 Adjustment of Weibull curves for Al–Al with a 9 mm bolt head radius.

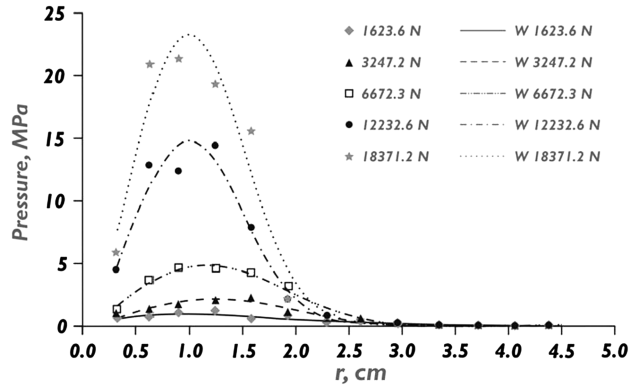

Fig. 9 Adjustment of Weibull curves for SS–SS with a 5 mm bolt head radius.

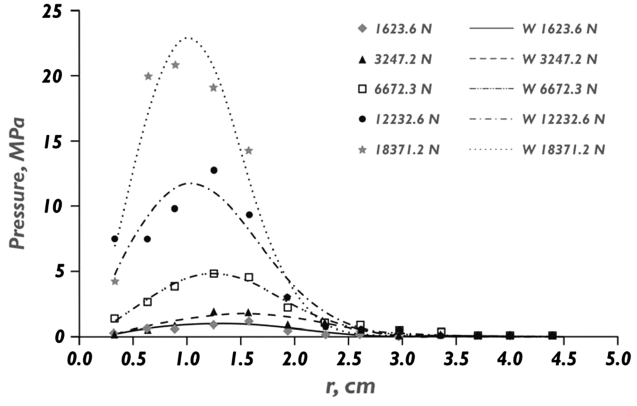

Fig. 10 Adjustment of Weibull curves for SS–SS with a 9 mm bolt head radius.

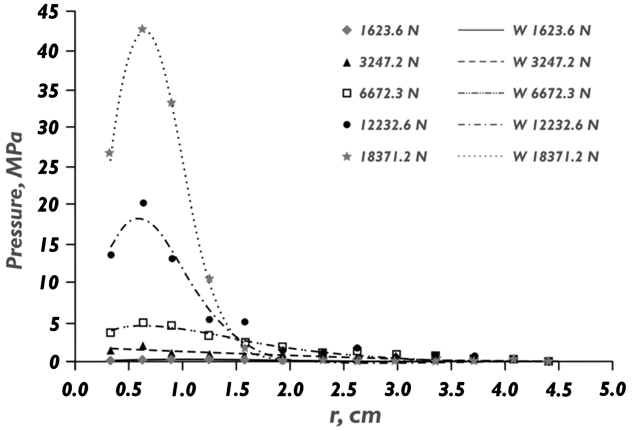

Fig. 11 Adjustment of Weibull curves for Al–SS with a 5 mm bolt head radius.

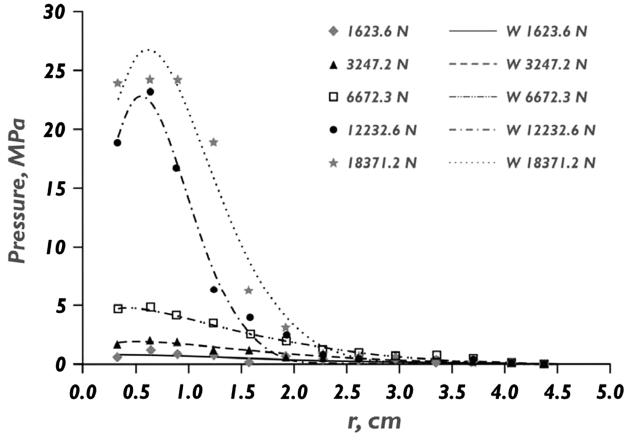

Fig. 12 Adjustment of Weibull curves for Al–SS with a 9 mm bolt head radius.

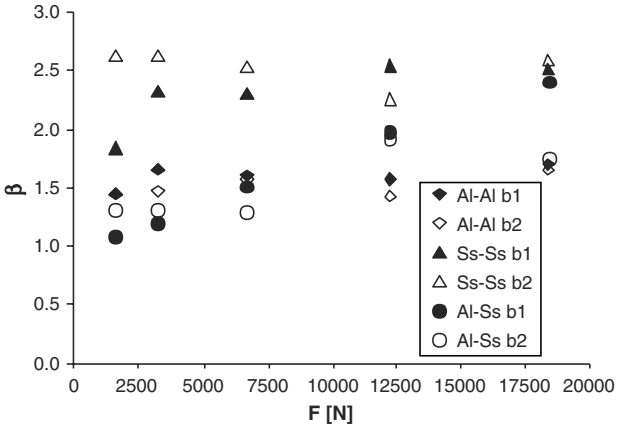

Fig. 14 Weibull β-coefficient values ($b1 = 5$ mm bolt heat radius, $b2 =$ 9 mm bolt head radius).

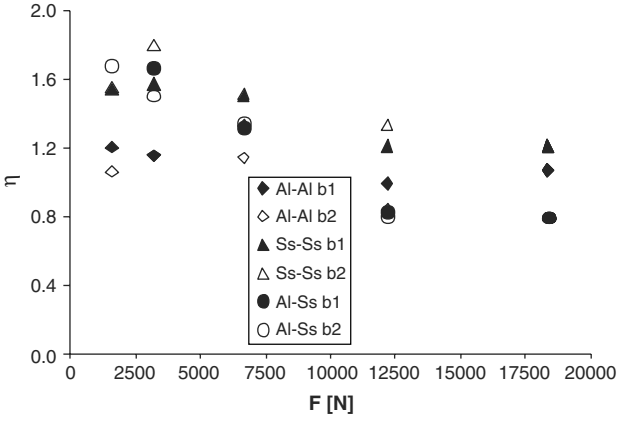

Fig. 15 Weibull η-coefficient values ($b1 = 5$ mm bolt heat radius, $b2 =$ 9 mm bolt head radius).

excellent comparison for light axial loads. For larger load levels, the comparison is not as good, especially near the bolt. However, the SS–SS data also show rapid slope variations near the bolt, which are predicted by the model (contrary to the Al–Al data, which shows a smoother slope variation). Comparing the Al–Al and SS–SS results, one can see that, for the SS–SS data, the peaks of the pressure distribution curves are displaced further away from the bolt than the Al–Al's. This could be due to the elastic deformation of the plates. The stainless steel plates are more rigid than the aluminum plates.

Figures 11 and 12 shows the Al–SS joint data for the bolt head radii of 5 and 9 mm, respectively. It is observed that the Weibull curves fit the data well for the entire range of axial loads and radius r. One can observe that, for these data sets, the peaks of the pressure distribution curves are located near the bolt, like the Al–Al data. This is an indication that the deformation of the aluminum plate, which is the less rigid of the two materials, is controlling the position of the pressure distribution curve peak.

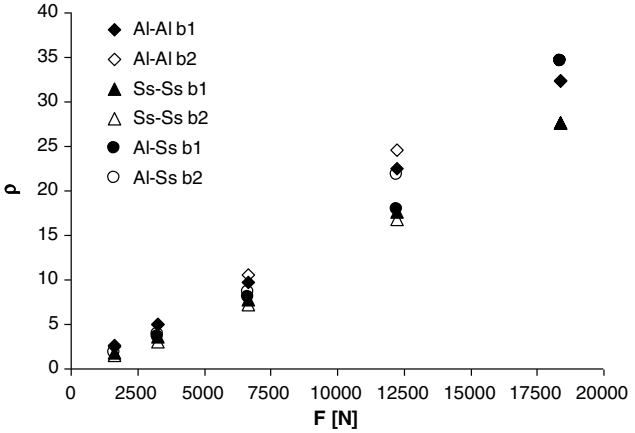

Fig. 13 Weibull ρ-coefficient values ($b1 = 5$ mm bolt heat radius, $b2 =$ 9 mm bolt head radius).

The values of the Weibull parameters ρ, β, and η that lead to the best fit to the data sets are presented in Figs. 13–15, respectively. The parameter ρ (Fig. 13) is associated to the Weibull curve amplitude, as already mentioned. As one can see, it increases approximately linearly with the applied axial force. For a given axial load, the ρ values are scattered within $\pm 20\%$ of the average. The parameter β (Fig. 14) does not show a clear trend with respect to the applied load: in some data sets, β is almost constant, whereas, for the Al–SS joint with the smaller bolt, it increases linearly. In general, the values scatter within $\pm 50\%$ of the average for the lightest load and $\pm 25\%$ for the largest load. Finally, the parameter η (Fig. 15) values scatter within $\pm 30\%$ of the average for a given axial load. In general, it decreases with the increasing load.

Conclusions

This work shows that the use of the Weibull probability density function to describe the shape of the contact pressure distribution of bolted joints looks very promising. The correlations showed a very good agreement with the experimental data. The Weibull function has been widely used in engineering to predict component life times. The model seems to predict the trend of the pressure distribution of bolted joints very well: a slight increase from a finite value at the bolt hole until a maximum value, followed by a smooth and near-exponential decrease before vanishing far from the bolt. The output

of the pressure-sensitive film is related to the likely end of life of an ink bubble, which in turn is more likely to happen near the bolt. The Weibull distribution then seems to be an adequate choice to describe the pressure levels as a function of the distance from the bolt.

The bolted joint pressure distribution data obtained using sensitive films available commercially had to be corrected, so that the obtained pressure distribution yields the bolt axial load and so the distribution drops to zero far from the bolt. Therefore, the sensitive films should be seen as a qualitative way to assess the interfacial pressure distribution. With the corrections introduced to the measured profile, the resulting curve shape seems to be consistent with previous works from the literature. The resulting shape of the measured pressure distribution is well predicted by the Weibull function.

The Weibull function used here has three parameters. One of them, related to the curve amplitude, increases linearly with the axial load applied by the bolt, whereas the other two parameters did not seem to present a well-defined trend with the axial load. Further studies are needed in order to estimate the Weibull parameters as a function of the joint characteristics and the axial load. Should the parameters be determined as a function of bolted joint parameters and axial load, one would be able to develop a single correlation for the pressure distribution of any kind of bolted joints.

A deeper study of the behavior of the Weibull statistical function should be performed. The focus should be on the influence of the geometrical and mechanical properties of the bolted joint on the Weibull parameters. A more comprehensive experimental work should be employed in this case, with wider ranges of joint parameters. Also, for future developments, other measurement techniques, such as the ultrasound waves, could also be employed.

References

[1] Fernlund, I., "A Method to Calculate the Pressure Between Bolted or Riveted Plates," *Transactions of Chalmers University of Technology*, No. 245, 1961.

[2] Motosh, N., "Determination of Joint Stiffness in Bolted Connections," *Journal of Engineering for Industry*, Vol. 98, No. 3, 1976, pp. 858–861.

[3] Motosh, N., "Stress Distribution in Joints of Bolted or Riveted Connections," *Journal of Engineering for Industry*, Vol. 97, No. 1, 1975, pp. 157–161.

[4] Chandrashekhara, K., and Muthanna, S. K., "Stress in Thick Plate with a Circular Hole under Axisymmetric Loading," *International Journal of Engineering Science*, Vol. 15, No. 2, 1977, pp. 135–146. doi:10.1016/0020-7225(77)90029-5

[5] Chandrashekhara, K., and Muthanna, S. K., "Pressure Distribution in Bolted Connections," *Advances in Reliability and Stress Analysis*, ASME Winter Annual Meeting, American Society of Mechanical Engineers, New York, Dec. 1978, pp. 117–124.

[6] Chandrashekhara, K., and Muthanna, S. K., "Analysis of a Thick Plate with a Circular Hole Resting on a Smooth Rigid Bed and Subjected to Axisymmetric Normal Load," *Acta Mechanica*, Vol. 33, Nos. 1–2, 1979, pp. 33–44. doi:10.1007/BF01175937

[7] Marshall, M. B., Lewis, R., and Dwyer-Joyce, R. S., "Characterisation of Contact Pressure Distribution in Bolted Joints," *Strain*, Vol. 42, No. 1, 2006, pp. 31–43. doi:10.1111/j.1475-1305.2006.00247.x

[8] Gould, H. H., and Mikic, B. B., "Areas of Contact Pressure Distribution in Bolted Joints," *Journal of Engineering for Industry*, Vol. 94, Nov.–Dec. 1971, pp. 864–870.

[9] Madhusudana, C. V., Peterson, G. P., and Fletcher, L. S., "The Effect of Nonuniform Interfacial Pressures on the Heat Transfer in Bolted and Riveted Joints," *Journal of Energy Resources Technology*, Vol. 112, No. 3, 1990, pp. 174–182. doi:10.1115/1.2905755

[10] Ito, Y., Toyoda, J., and Nagata, S., "Interface Pressure Distribution in Bolt Flange Assembly," *Journal of Mechanical Design*, Vol. 101, No. 4, 1979, pp. 330–337.

[11] Mittelbach, M., Vogd, C., Fletcher, L. S., and Peterson, G. P., "The Interfacial Pressure Distribution and Thermal Conductance of Bolted Joints," *Journal of Heat Transfer*, Vol. 116, No, 4, 1994, pp. 823–828. doi:10.1115/1.2911454

[12] Pau, M., Baldi, A., and Leban, B., "Visualization of Contact Areas in Bolted Joints Using Ultrasonic Waves," *Experimental Techniques*, Vol. 32, No. 4, 2008, pp. 49–53. doi:10.1111/j.1747-1567.2007.00265.x

[13] Sawa, T., Kumano, H., and Morohoshi, T., "The Contact Stress in a Bolted Joint with a Threaded Bolt," *Experimental Mechanics*, Vol. 36, No. 1, March 1996, pp. 17–23. doi:10.1007/BF02328693

[14] Meyer, P. L., "*Probabilidade: Aplicações à Estatística*," 2nd Ed., Livros Técnicos e Científicos Editora, Rio de Janeiro, Brazil, 1995.